

Albisporachelin, a New Hydroxamate Type Siderophore from the Deep Ocean Sediment-Derived Actinomycete *Amycolatopsis albispora* WP1^T

Qihao Wu ^{1,§}, Robert W. Deering ^{2,§}, Gaiyun Zhang ³, Bixia Wang ¹, Xin Li ¹, Jiadong Sun ², Jianwei Chen ¹, Huawei Zhang ¹, David C. Rowley ^{2,*} and Hong Wang ^{1,*}

¹ College of Pharmaceutical Science, Zhejiang University of Technology, Hangzhou 310014, Zhejiang, China; hongw@zjut.edu.cn

² Department of Biomedical and Pharmaceutical Science, College of Pharmacy, University of Rhode Island, Kingston, Rhode Island 02881, United States; drowley@uri.edu

³ Key Laboratory of Marine Biogenetic Resources, Third Institute of Oceanography, State Oceanic Administration, Xiamen 361005, Fujian, China.

* Correspondence: hongw@zjut.edu.cn; Tel.: +86-571-8832-0622; drowley@uri.edu; Tel.: 401-874-9228

† These authors contributed equally to this work.

Table of contents

Figures

Figure S1. Colony morphology of *A. albispora* WP1^T on ISP₂ agar plate

Figure S2. The 16S rRNA phylogram of representative *Amycolatopsis* strains

Figure S3. CAS activity guided isolation of siderophore from the supernatant extract of *A. albispora* WP1^T

Figure S4. HR-ESI-MS spectrum of albisorachelin in negative mode

Figure S5. ¹H NMR spectrum of albisorachelin in DMSO-*d*₆

Figure S6. ¹³C NMR spectrum of albisorachelin in DMSO-*d*₆

Figure S7. FT-IR-spectrum of albisorachelin

Figure S8. ¹H- ¹H COSY spectrum of albisorachelin in DMSO-*d*₆

Figure S9. TOCSY spectrum of albisorachelin in DMSO-*d*₆

Figure S10. HSQC spectrum of albisorachelin in DMSO-*d*₆

Figure S11. HMBC spectrum of albisorachelin in DMSO-*d*₆

Figure S12. NOESY spectrum of albisorachelin in DMSO-*d*₆

Figure S13. Observed main fragments list of compound **1** during MS² fragmentation experiments

Figure S14. Main fragments observed during MS² fragmentation experiments and assignment of the molecular ion peak

Figure S15. HPLC trace of FDAA-derivatized albisorachelin hydrolysate with standard

Figure S16. LC-MS-traces of FDAA-derivatized albisorachelin hydrolysate

Figure S17. MS spectrum of mono- α N-Me-L-Orn-L-FDAA in albisorachelin hydrolysate

Figure S18. MS spectrum of mono- α L-Orn-L-FDAA in albisorachelin hydrolysate

Figure S19. MS spectrum of mono- ω L-Orn-L-FDAA in albisorachelin hydrolysate

Figure S20. MS spectrum of mono- ω N-Me-L-Orn-L-FDAA in albisorachelin hydrolysate

Figure S21. MS spectrum of L-Ser-L-FDAA in albisorachelin hydrolysate

Figure S22. UV-visible spectra of albisorachelin and ferric complex of albisorachelin

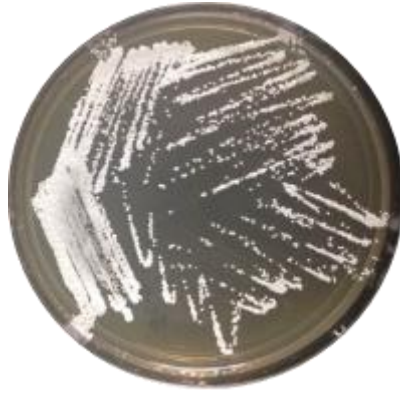


Figure S1. Colony morphology of *A. albispora* WP1^T on ISP₂ agar plate.

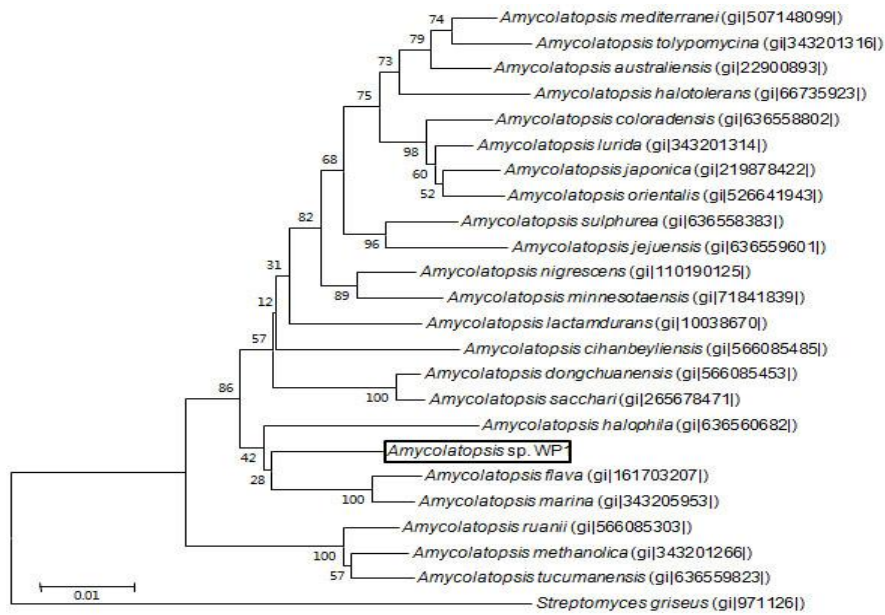


Figure S2. The 16S rRNA phylogram of representative *Amycolatopsis* strains. With an outgroup containing *S. griseus*. Ribosomal RNA sequences for all strains but *A. albispora* WP1^T were obtained from GenBank database.

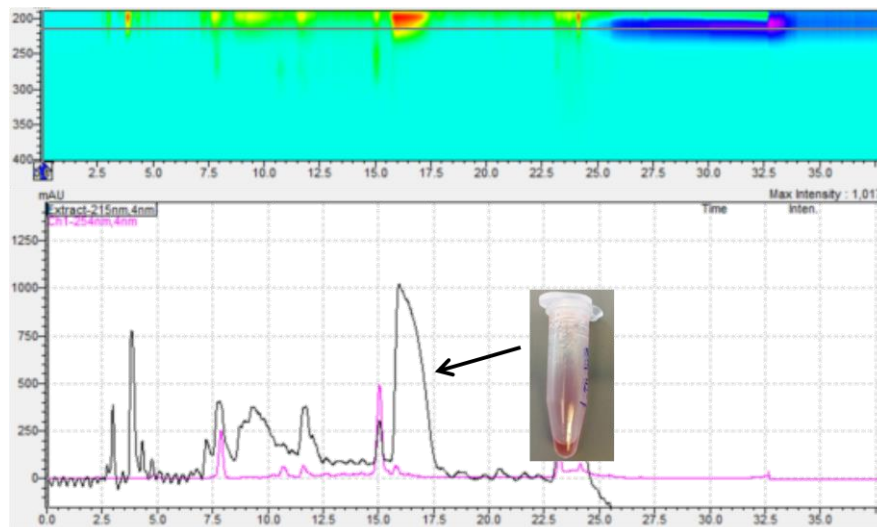


Figure S3. CAS activity guided isolation of siderophore from the supernatant extract of *A. albispora* WP1^T.

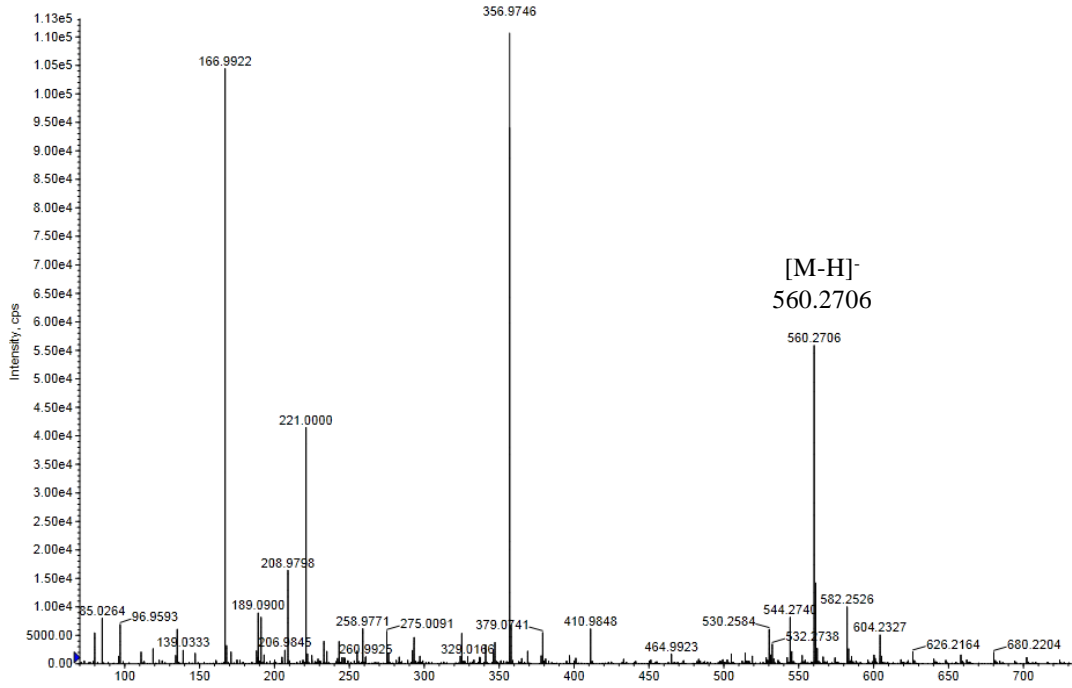


Figure S4. HR-ESI-MS spectrum of albisorachelin in negative mode.

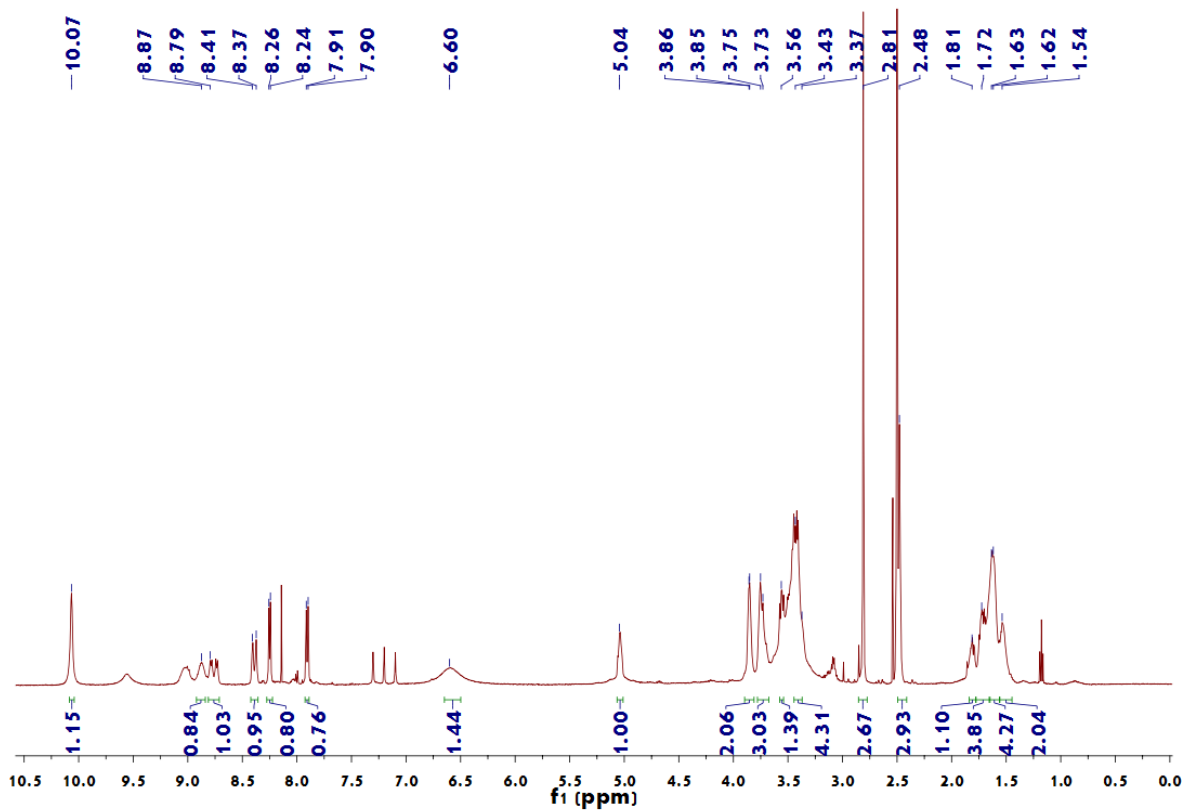


Figure S5. ¹H NMR spectrum of albisorachelin in DMSO-*d*₆.

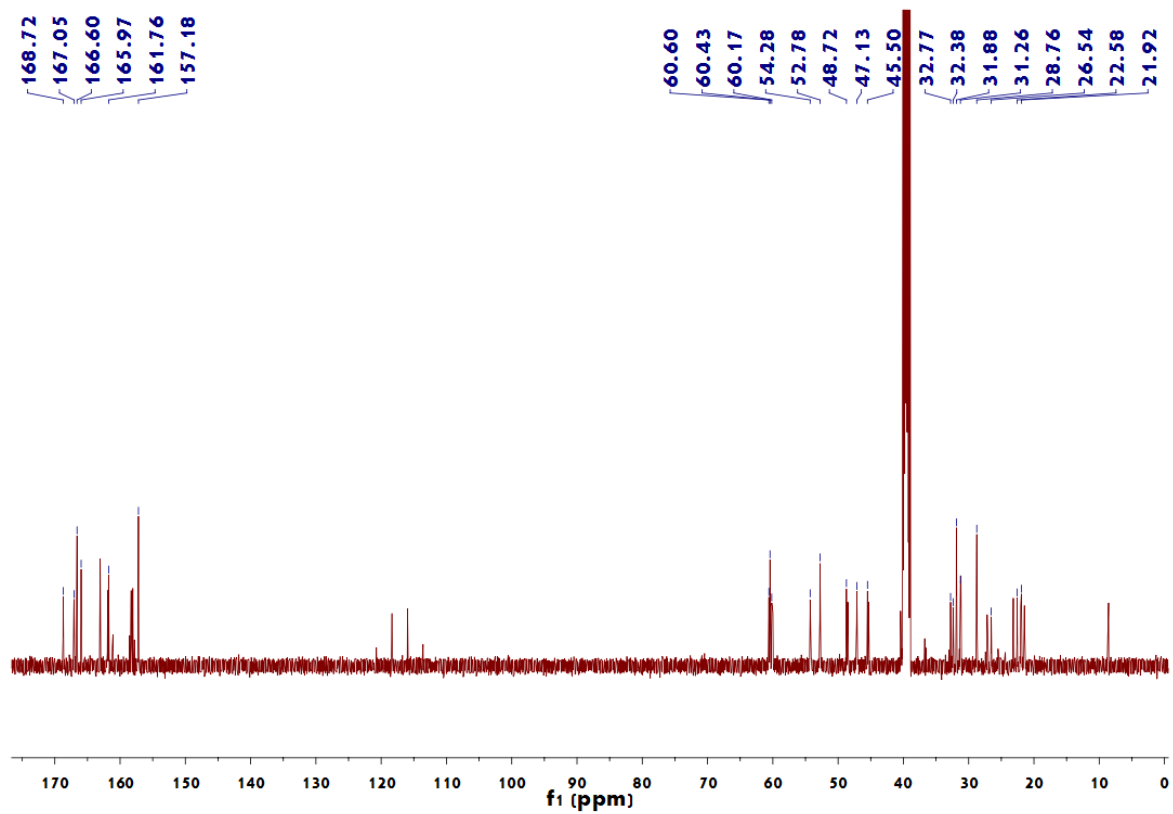


Figure S6. ^{13}C NMR spectrum of albisorachelin in $\text{DMSO-}d_6$.

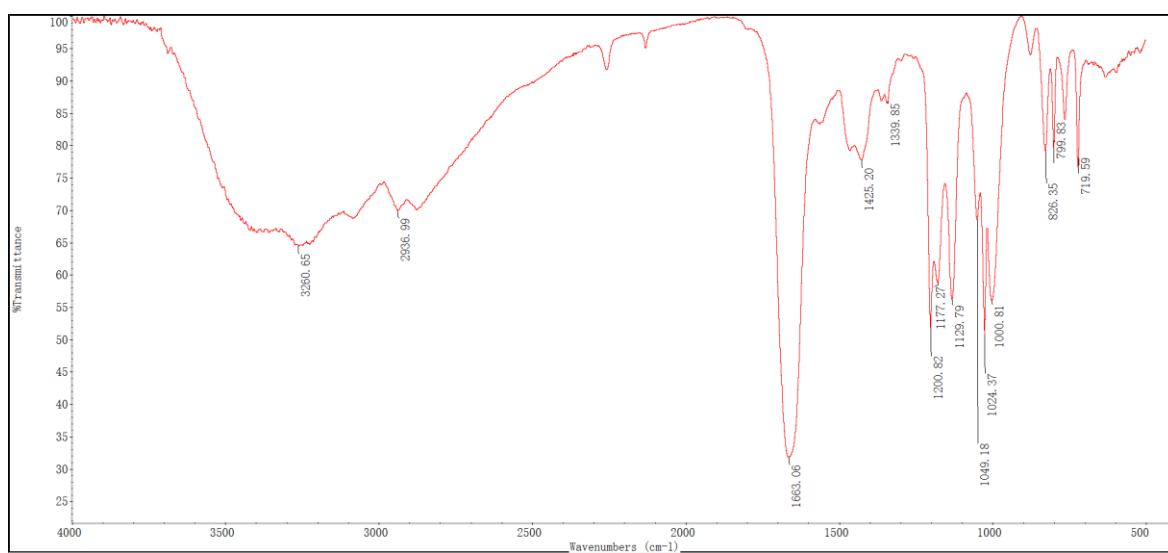


Figure S7. FT-IR-spectrum of albisorachelin.

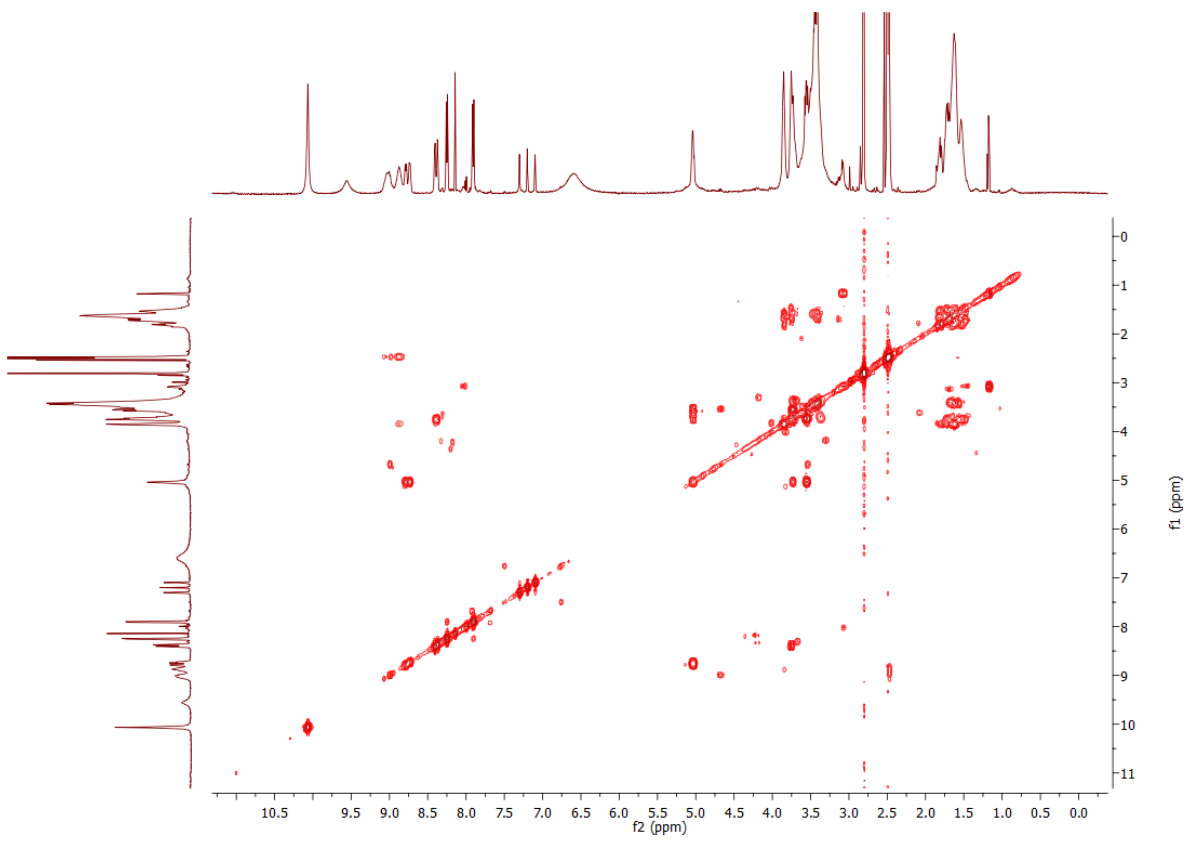


Figure S8. ^1H - ^1H COSY spectrum of albisorachelin in $\text{DMSO-}d_6$.

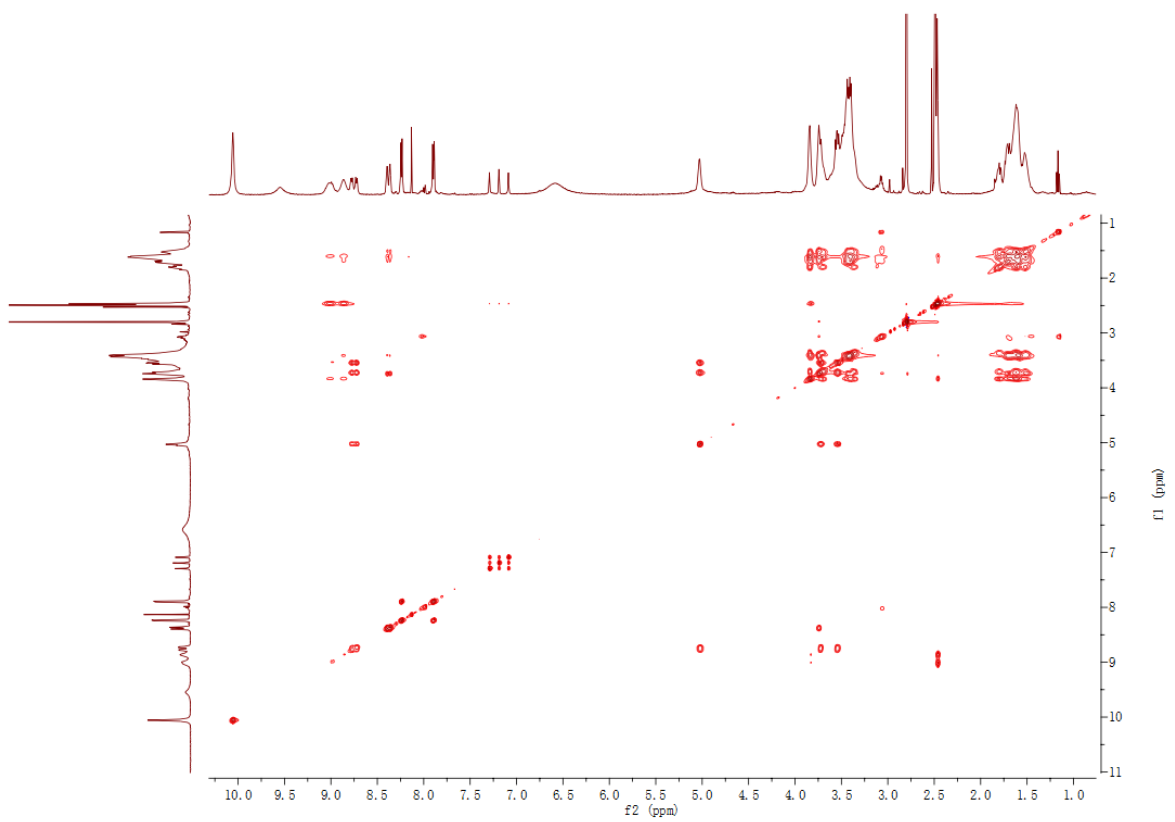


Figure S9. TOCSY spectrum of albisorachelin in $\text{DMSO-}d_6$.

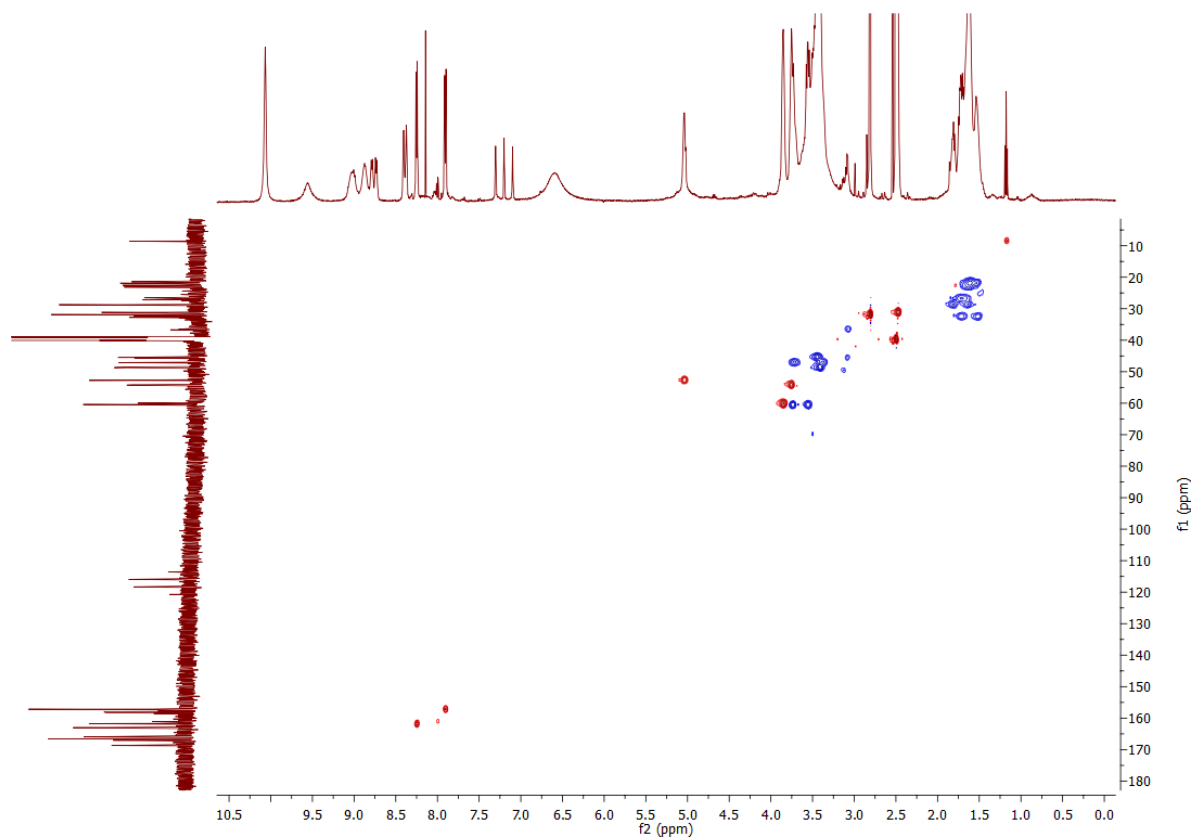


Figure S10. HSQC spectrum of albisorachelin in DMSO-*d*₆.

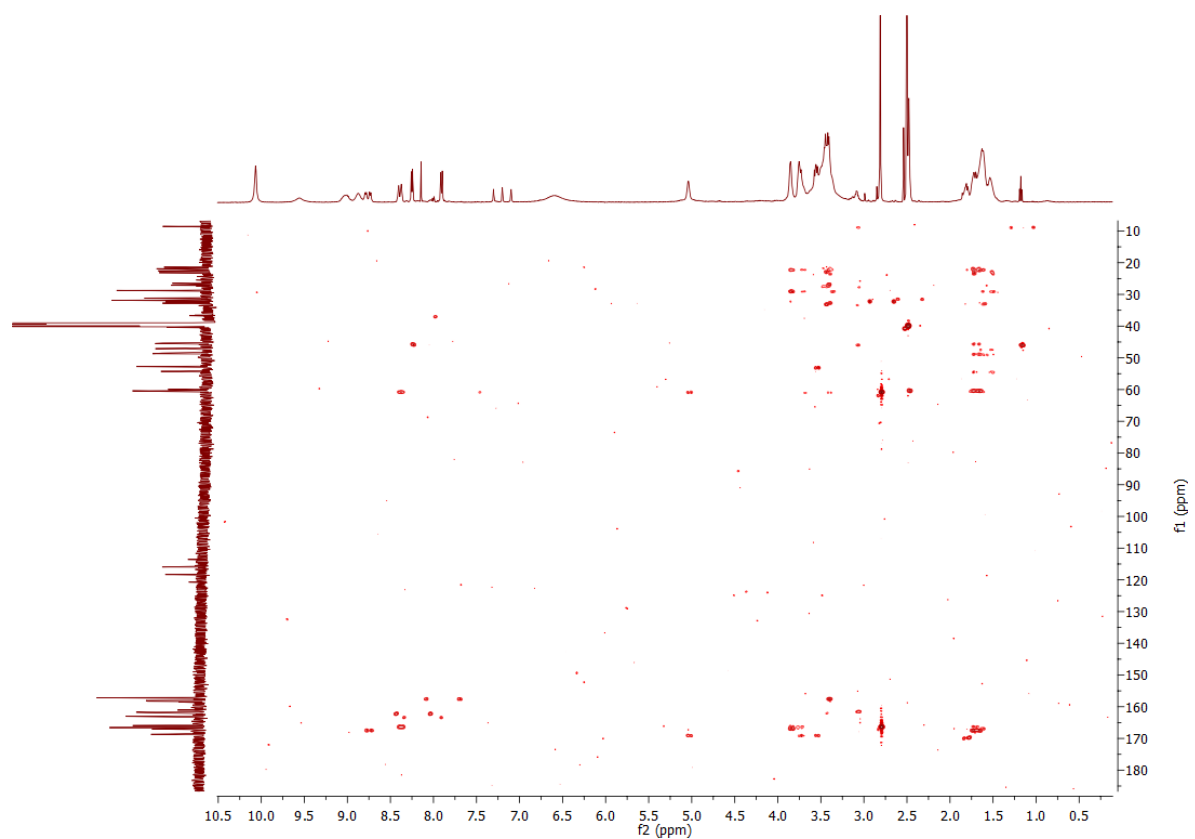


Figure S11. HMBC spectrum of albisorachelin in DMSO-*d*₆.

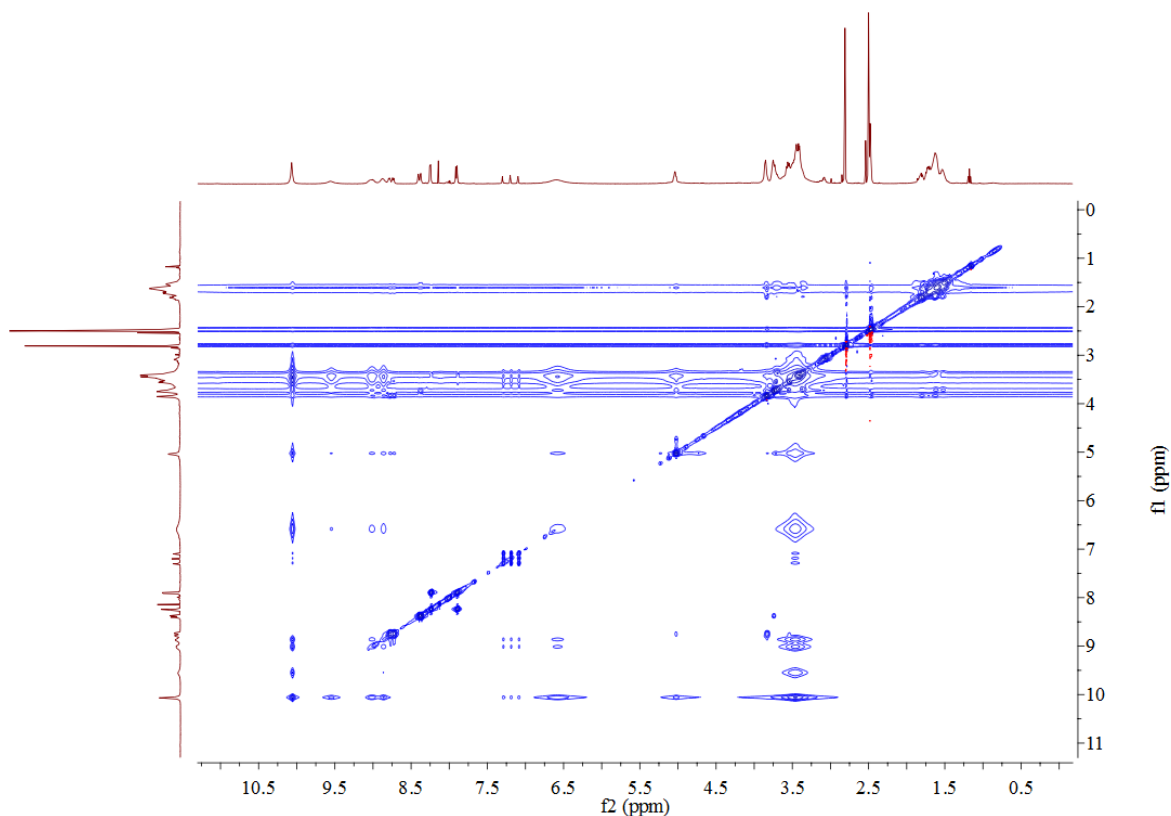


Figure S12. NOESY spectrum of albispochelin in DMSO-*d*₆.

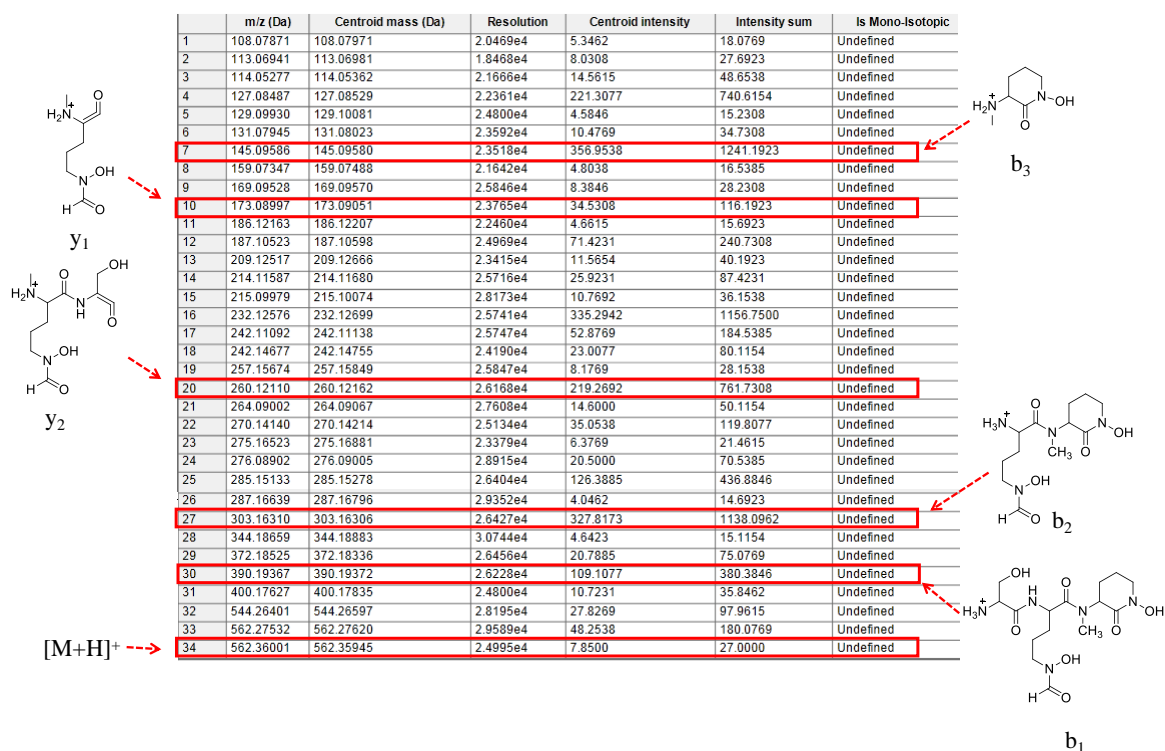


Figure S13. Observed main fragments list of compound 1 during MS² fragmentation experiments.

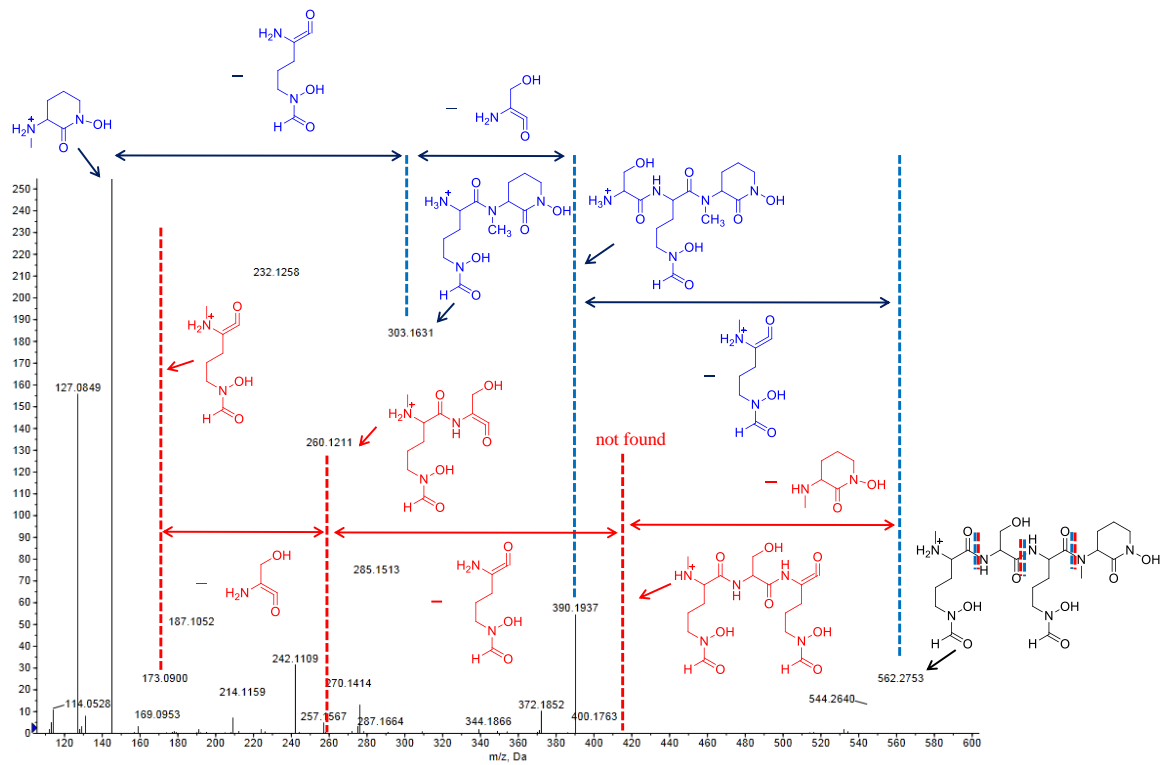


Figure S14. Main fragments observed during MS² fragmentation experiments and assignment of the molecular ion peak.

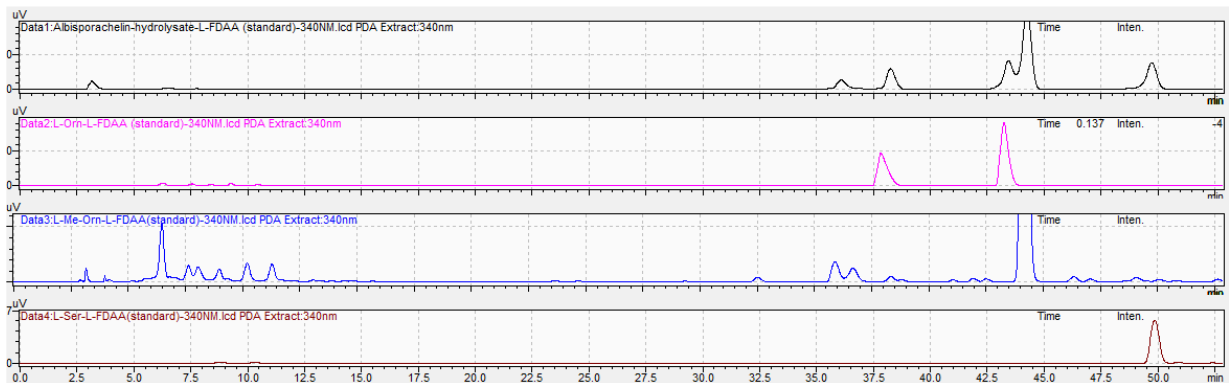


Figure S15. HPLC trace of FDAA-derivatized albisporchelin hydrolysate with standard. Trace A is albisporchelin hydrolysate; trace B is standard L-Orn-L-FDAA; trace C is standard L-Me-Orn-L-FDAA; trace D is standard L-Ser-L-FDAA.

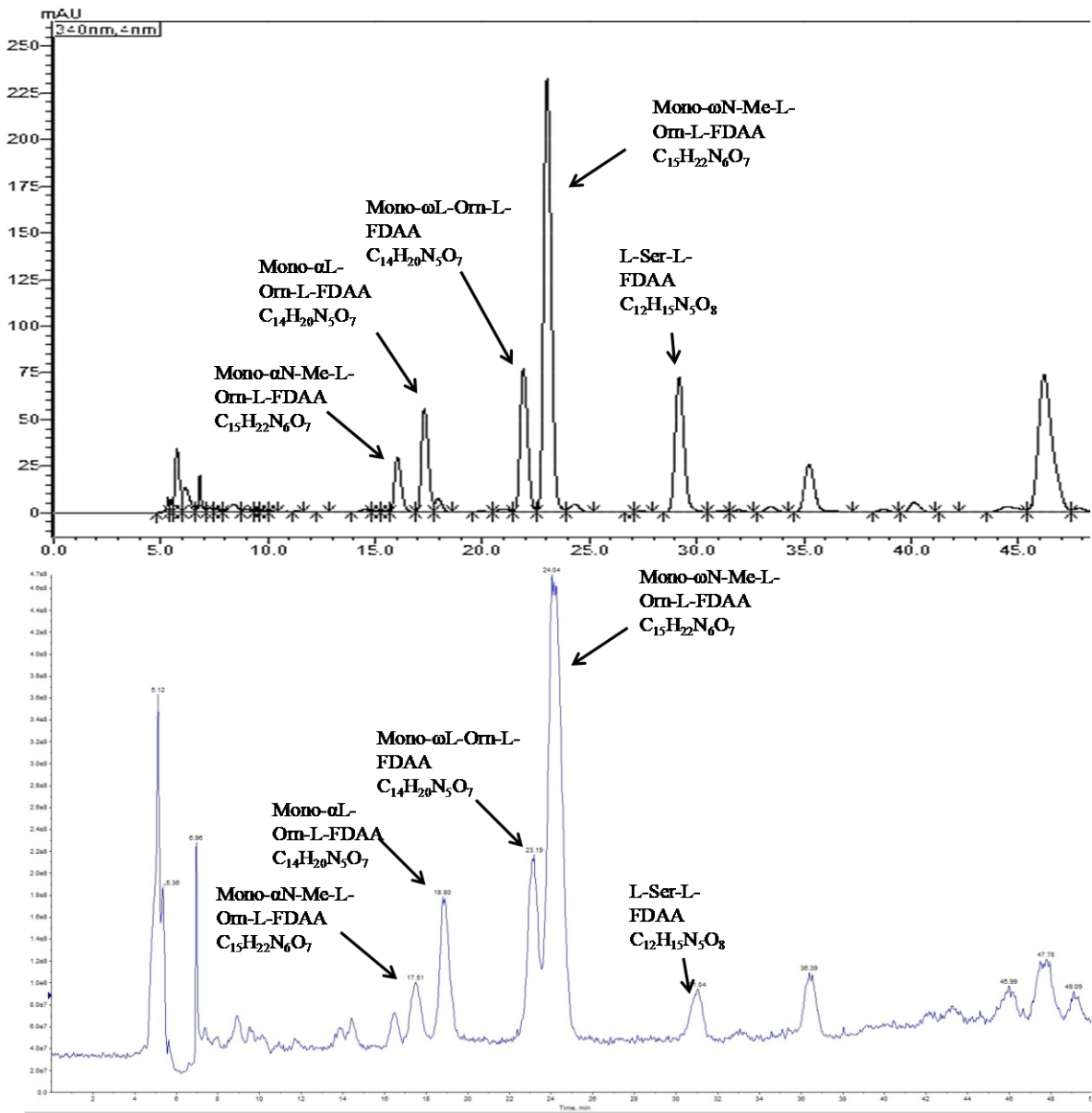


Figure S16. LC-MS-traces of FDAA-derivatized albisporachelin hydrolysate.

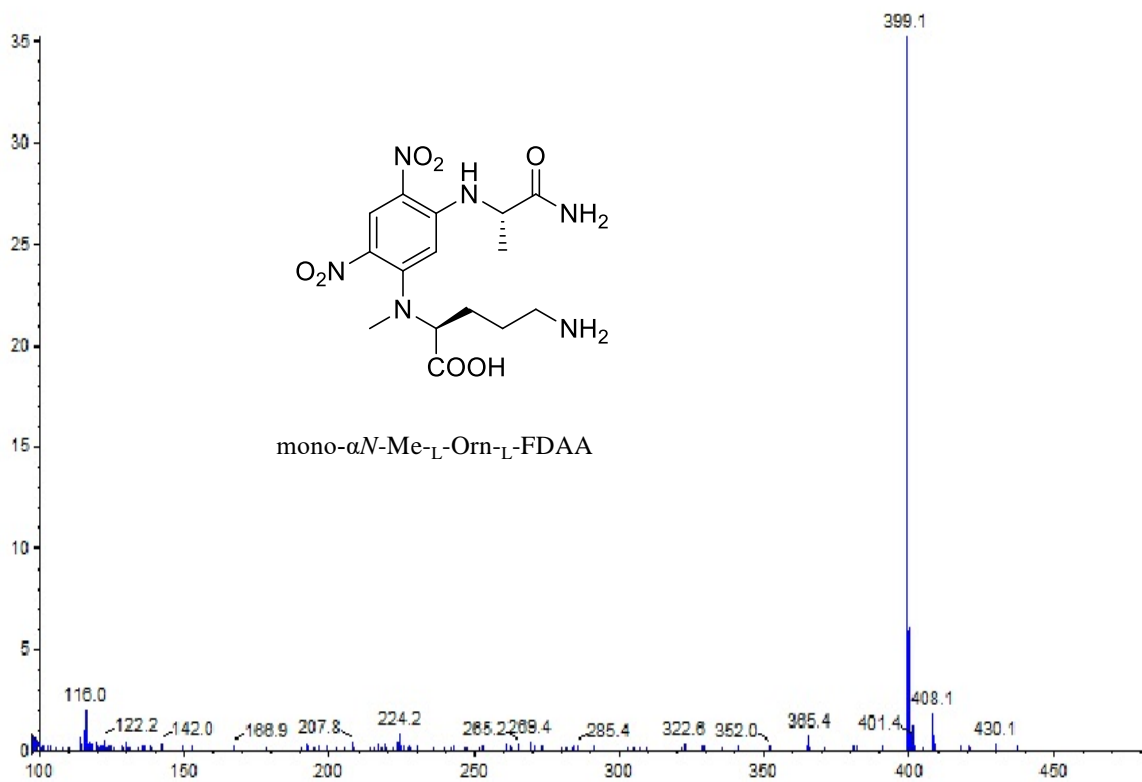


Figure S17. MS spectrum of mono- α N-Me-L-Orn-L-FDAA in albisorachelin hydrolysate.

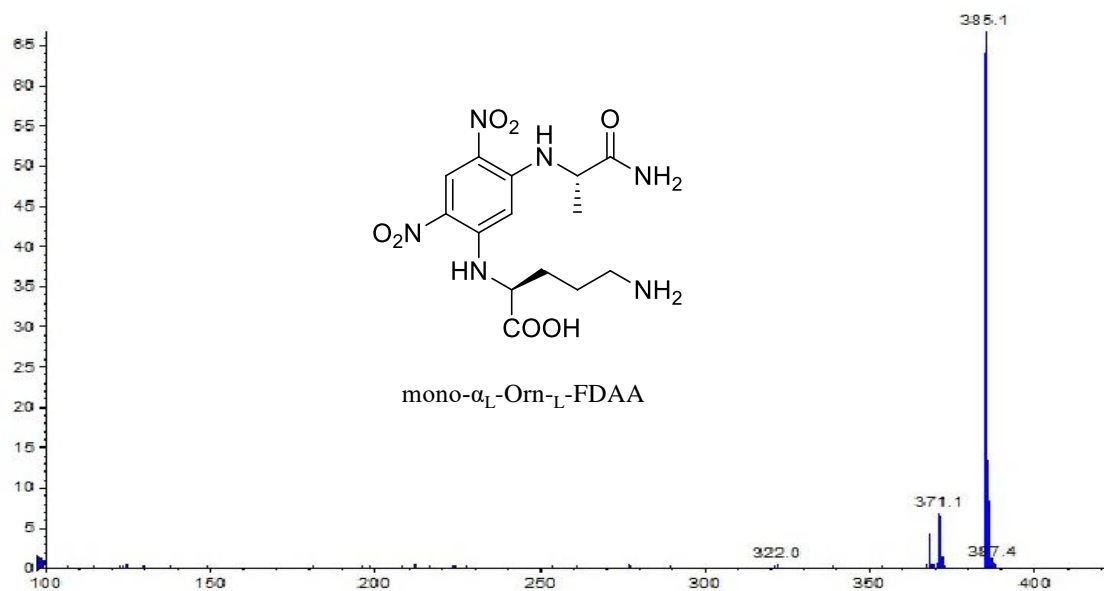


Figure S18. MS spectrum of mono- α L-Orn-L-FDAA in albisorachelin hydrolysate.

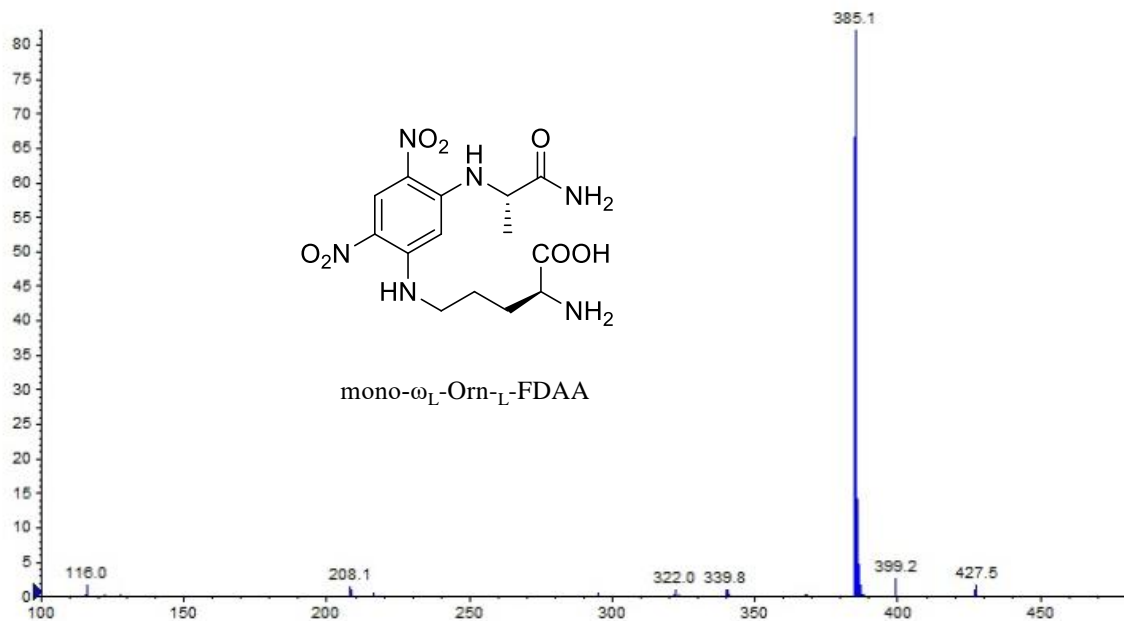


Figure S19. MS spectrum of mono- ω -L-Orn-L-FDAA in albisorachelin hydrolysate.

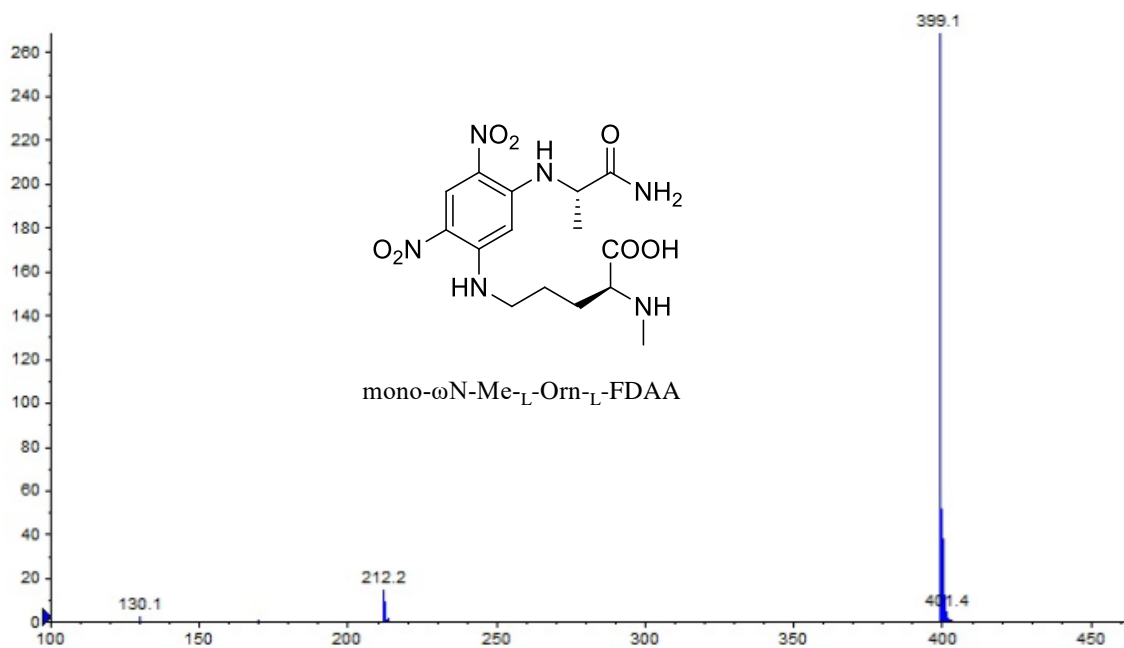


Figure S20. MS spectrum of mono- ω -N-Me-L-Orn-L-FDAA in albisorachelin hydrolysate.

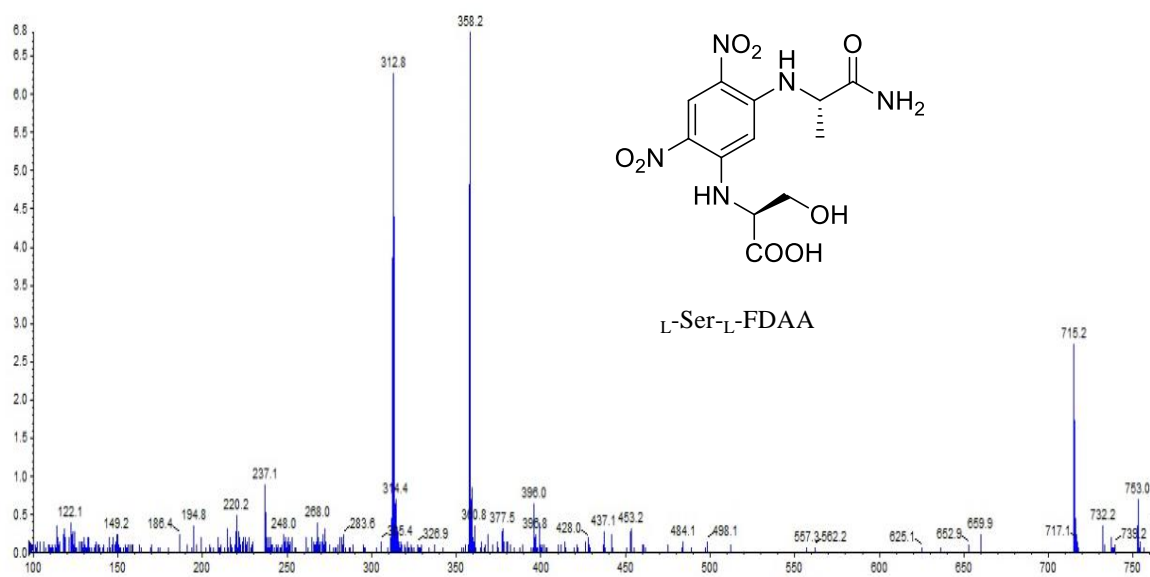


Figure S21. MS spectrum of L-Ser-L-FDAA in albiporachelin hydrolysate.

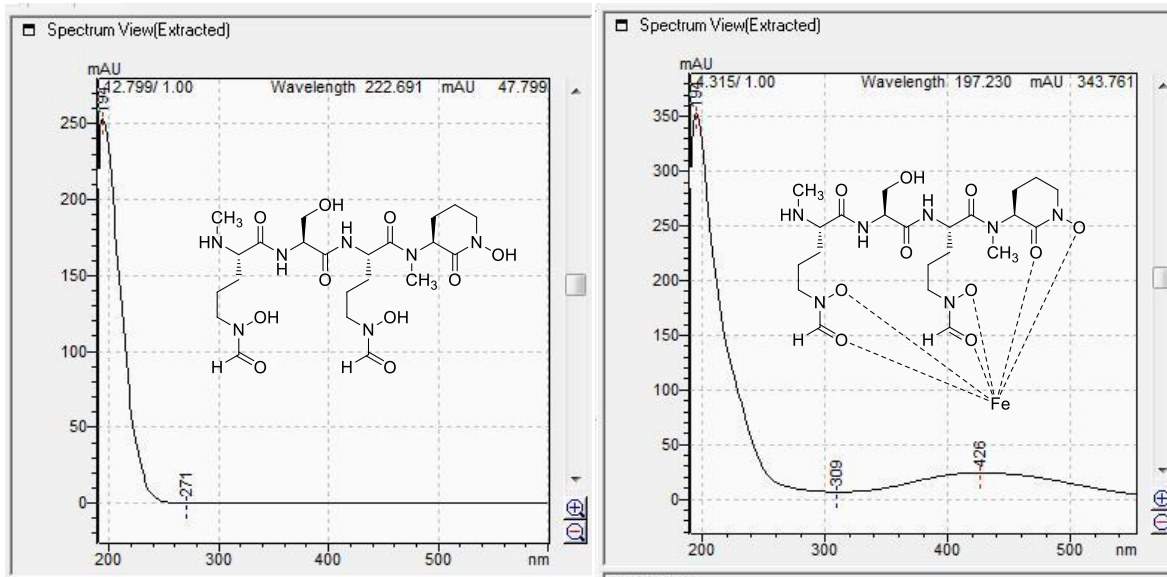


Figure S22. UV-visible spectra of albiporachelin and ferric complex of albiporachelin.